Accepted Manuscript

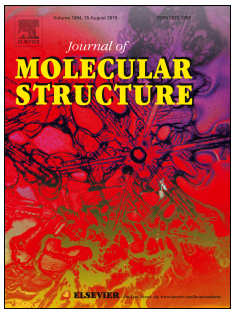

Synthesis, spectral characterization, crystal structure and molecular docking study of 2,7-diaryl-1,4-diazepan-5-ones

S. Sethuvasan, P. Sugumar, V. Maheshwaran, M.N. Ponnuswamy, S. Ponnuswamy

PII: S0022-2860(16)30218-6

DOI: 10.1016/j.molstruc.2016.03.021

Reference: MOLSTR 22332

To appear in: *Journal of Molecular Structure*

Received Date: 26 January 2016

Revised Date: 5 March 2016

Accepted Date: 7 March 2016

Please cite this article as: S. Sethuvasan, P. Sugumar, V. Maheshwaran, M.N. Ponnuswamy, S. Ponnuswamy, Synthesis, spectral characterization, crystal structure and molecular docking study of 2,7-diaryl-1,4-diazepan-5-ones, *Journal of Molecular Structure* (2016), doi: 10.1016/j.molstruc.2016.03.021.

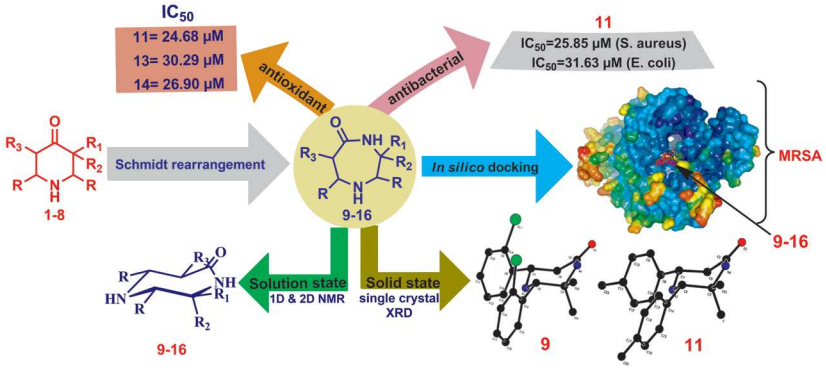

Synthesis, spectral characterization, crystal structure and molecular docking study of 2,7-diaryl-1,4-diazepan-5-ones

S. Sethuvasan[a], P. Sugumar[b], V. Maheshwaran[b], M. N. Ponnuswamy[b] and S. Ponnuswamy[a]*

[a]*P.G. & Research Department of Chemistry, Government Arts College (Autonomous), Coimbatore - 641 018, India.*

[b]*Centre of Advanced Study in Crystallography and Biophysics, University of Madras, Guindy Campus, Chennai - 600 025, India.*

Abstract

In this study, a series of variously substituted *r*-2,*c*-7-diaryl-1,4-diazepan-5-ones **9**-**16** have been synthesized using Schmidt rearrangement and are characterized by IR, mass and 1D & 2D NMR spectral data. The proton NMR coupling constant and estimated dihedral angles reveal that the compounds **9**-**16** prefer a chair conformation with equatorial orientation of alkyl and aryl groups. Single crystal X-ray structure has been solved for compounds **9** and **11** which also indicates the preference for distorted chair conformation with equatorial orientation of substituents. The compounds **9**-**16** have been docked with the structure of Methicillin-resistant Staphylococcus aureus (MRSA) and the results demonstrate that compound **10** is having better docking score and glide energy than others and it is comparable to co-crystal ligand. Furthermore, all the compounds have been evaluated for their antibacterial and antioxidant activities. All the compounds show moderate antibacterial activity and only **11** exhibits better activity against *S. aures* and *E. coli*. The compounds **11**, **13** and **14** exhibit half of the antioxidant power when compared to the BHT and the remaining compounds show moderate activity.

Keywords: 2,7-diaryl-1,4-diazepan-5-ones, Chair conformation, Single crystal XRD, Molecular docking, Antibacterial, Antioxidant.

*Corresponding author: Post Graduate and Research Department of Chemistry, Government Arts College (Autonomous), Coimbatore-641 018, Tamil Nadu, India. Mobile number: +919244645744, E-mail: kspons2001@gmail

1. Introduction

ε-Caprolactam plays an important role for the preparation of modified nylons [1] and nanogels [2]. The 1,4-diazepanone ring nucleus acts as anticonvulsant agent and is present in the liposidomycin nucleoside antibiotics that inhibits bacterial peptidoglycan synthesis [3]. Furthermore, recent studies on 1,4-diazepan-5-ones reveal their antimicrobial [4], antitrypanosomal and antiplasmodial activities [5]. However, a little information is only available on the synthesis, stereochemistry and biological evaluation of 2,7-diaryl-1,4-diazepan-5-ones. Hence, it is of interest to report the synthesis and characterisation of 2,7-diaryl-1,4-diazepan-5-ones by the ring expansion of 2,6-diarylpiperidin-4-ones using Schmidt rearrangement. Only a few 2,7-diaryl-1,4-diazepan-5-ones have been already reported using Beckmann rearrangement of piperidin-4-ones oximes [4, 6, 7] as well as Schmidt rearrangement of piperidin-4-ones [8-16].

The present work involves the synthesis of a new series of 2,7-diaryldiazepan-5-ones **9**-**16** from their corresponding piperidin-4-ones **1**-**8** using Schmidt rearrangement with a modified procedure (Scheme 1). Earlier the Schmidt rearrangement of piperidin-4-ones have been carried out in two steps *i.e.* converting piperidin-4-ones into hydrochlorides and subjecting them to Schmidt rearrangement after isolation [8, 11-14]. The conversion in one step with simple reaction conditions is reported now.

The structural characterization and analysis of solution state conformation are made using IR, mass, 1D and 2D NMR spectral studies. Furthermore, the X-ray crystal structures of **9** and **11** have been solved in order to confirm their preferred conformation in solid state. Baliah *et. al*. [6] reported only the synthesis of diazepan-5-one **12** from its oxime derivative of piperidin-4-one by Beckmann rearrangement. However, the spectral data and stereochemistry of **12** have not been reported. Depending on the migratory aptitude of the C-3 and C-5 carbons in piperidin-4-ones **1**-**8**, two kinds of isomers are possible for the products in the Schmidt rearrangements. The spectral data of earlier studies [8, 11] confirmed the migration of C-3 to form diazepan-5-ones **9**-**16** as expected product. All the synthesised compounds have been tested for their antibacterial and antioxidant activities. In addition, molecular docking studies have been carried out for compounds **9**-**16**. The docking studies show that the compounds inhibit at the active site of the target protein and can be utilized as potential drug molecules.

2. Experimental

2.1. Materials and methods

All the reported melting points which are uncorrected have been taken in open capillaries using melting point apparatus with a calibrated thermometer. FT-IR spectra have been recorded on a Bruker alpha spectrophotometer using KBr pellets. ^{1}H and ^{13}C NMR spectra have been recorded in $CDCl_3$ and DMSO-d_6 on a Bruker NMR spectrometer (400 & 500 MHz for ^{1}H and 100 & 125 MHz for ^{13}C), using TMS as internal standard. Chemical shifts (δ) are expressed in ppm where abbreviations s, bs, d, dd, and m stand for the resonance multiplicities singlet, broad singlet, doublet, doublet of doublet and multiplet, respectively, and coupling constants are given in Hz. Electron impact mass spectra have been recorded using JEOL GCMS spectrometer. Elemental analyses have been carried out in Carlo Erba 1108 CHN analyzer and are within 0.4% of the calculated values.

All the parent *r*-2,*c*-6-diarylpiperidin-4-ones **1-8** have been prepared according to the reported procedures [17].

*2.2. General procedure for the synthesis of r-2,c-7-diaryl[1,4]diazepan-5-ones **9-16**.*

r-2,*c*-6-Diarylpiperidin-4-ones **1-8** (0.03 mol) in conc. HCl (2 ml) and dichloromethane (60 ml) are stirred well in a beaker for a few minutes. To this stirred solution, conc. H_2SO_4 (20 ml) is added in dropwise at 0-5 ºC for 1 h. Temperature of the solution is allowed to rise at 25 ºC. While stirring, NaN_3 (0.09 mol) is added over a period of 1h and stirring is continued for another 2-3 h. The solution is poured into crushed ice and stirred well. Ammonium hydroxide is added slowly with stirring to reach pH=11. The resulting mass is washed with water and about 20 ml of dichloromethane is added. The organic layer is separated, dried over anhydrous Na_2SO_4 and concentrated for crystallization. The crystals thus obtained are recrystallized from dichloromethane-pet ether (60-80 ºC) in the ratio of 5:1.

2.3. Single crystal X-Ray studies

X-ray diffraction intensity data have been collected for the 2,7-diaryl-1,4-diazepan-5-ones **9** and **11** on Bruker axs Kappa ApexII [18] single crystal X-ray diffractometer

equipped with graphite mono-chromated MoKα (λ=0.7103 Å) radiation and CCD detector. Crystals have been cut to suitable size and mounted on a glass fibre using cyanoacrylate adhesive. The unit cell parameters have been determined from 36 frames measured (0.5° phi-scan) from three different crystallographic zones and using the method of difference vectors. An average four-fold redundancy per reflection has been used to collect the data at an optimum resolution of 0.75 Å. The intensity data collection, frames integrations (Lorentz and polarization) and decay correction have been done using SAINT-NT (version 7.06) [18] software. Empirical absorption correction (multi-scan) has been performed using SADABS [18] program. Crystal structures have been solved by direct methods using SHELXS-97 [19]. The phase sets with the best combined figure of merits reveal the positions of all non-hydrogen atoms in both the structures. The structures have been then refined by full-matrix least-squares procedures using SHELXL-97 [19].

2.4. Molecular docking studies

Molecular docking studies have been performed to examine the binding mode and pattern of ligands with MRSA, for which the structural coordinates have been retrieved from Protein Data Bank (PDB ID: 4D7I) [20]. The target protein is optimized after removal of the water molecules from the crystal structure and partial atomic charges assigned according to the force field. Minimization of target is performed until the average root mean square (rms) deviation of the non-hydrogen atoms reached 0.3 Å (OPLS-2005 force field) to remove the steric hindrance. Ligands are also minimized by OPLS-2005 force field. The results with the docking score are compared with the co-crystal ligand. The docking studies are carried out using Glide module of MAESTRO, Schrodinger suite [21]. The figures are generated using Pymol [22].

2.5. Antibacterial evaluation

2.5.1 Test Organisms

Four human pathogenic bacterial strains viz., *Staphylococcus aureus* (ATCC 25923), *Streptococcus pyogenes* (ATCC 19615), *Micrococcus luteus* (ATCC 9341) and *Escherichia coli* (ATCC 25922) have been maintained on nutrient agar slants at refrigerated condition until used in the present study.

2.5.2. Agar well diffusion method

Agar well diffusion method [23] has been followed to determine the antibacterial activity. Nutrient agar (NA) plates have been swabbed (sterile cotton swabs) with 8 hour old - broth culture of respective bacteria. The well, measuring 6 mm in diameter has been made in each of these plates using sterile cork borer. Each petri plate has been prepared by pouring 20 ml of appropriate agar media. The solutions of synthesized compounds **9-16** have been prepared at a concentration of 1 mg/ml using DMSO. About 100 µl solutions of each compound have been added into the wells of seeded plates. DMSO has been used as a control for all the experiments. The plates have been incubated at 37°C for 18-24 h and antibacterial activity has been determined by measuring the diameter of the inhibition zone and the activity index has also been calculated. Triplicates have been maintained and the experiment has been repeated thrice. For each replicates, the readings have been taken in three different fixed directions and the average values have been reported.

2.5.3. MIC using MTT assay method

The MTT assay has been carried out as described by Mosman [24]. The 96 wells plates have been prepared under aseptic conditions. Each culture plates have the volume of 100µl which contain Mueller Hinton Broth (MHB) and compounds **9-16** are dissolved with 5% (v/v) DMSO. Using micropipette, serially descending concentrations (400, 200, 100, 50, 25, 12.5 and 6.25 µg/ml) of compounds **9-16** have been prepared. A 10µl of bacterial suspension has been added to each well to achieve a density of 1.0×10^7 CFU/ml (McFarland No. 0.5). The commercial antibiotic ampicillin has been used as positive control. The plates have been placed in an incubator at 37 °C for 24 h. Then, to all these wells, 10 µl of MTT solution (5mg/ml of MTT in PBS) has been added. After 4 h, the medium has been discarded and added 150 µl of DMSO. The plates have been kept for 10 min in order to make the complete dissolution. Optical absorbance has been measured at 490 nm.

2.6. Antioxidant evaluation

2.6.1. DPPH radical scavenging assay

The evaluation of antioxidant activity of newly synthesized compounds has been done by DPPH radical scavenging activity (RSA) [25]. Solutions of all the synthesized compounds **9-16** have been prepared in different concentrations (50, 100, 200, 300, 400 and 500 µg/ml) using methanol. The 1 ml of test compounds solutions (**9-16**) has been added with 0.1 mM methanol solution of DPPH and shaken vigorously. The solution tubes have

been incubated at room temperature in dark room for 30 min. The decrease in absorbance has been measured at 517 nm using UV-Visible spectrophotometer and remaining DPPH has been calculated. Butylated Hydroxytoluene (BHT) has been used as standard and the experiment has been carried out in triplicate. From the results of this bioassay, RSA % has been calculated using the following formula:

$$\% \text{ Scavenging} = [(Ac-As)/Ac \times 100]$$

where Ac is the absorbance of the control and As is the absorbance of the compound.

3. Results and discussion

3.1. Analysis of IR and Mass spectra

The IR spectra of the diazepan-5-ones **9-16** display the bands at 3281-3322 cm^{-1} for amine NH and 3195-3216 cm^{-1} for amide NH. The strong band at 1651-1673 cm^{-1} is indicative of the amide CO stretching which in turn confirms the formation of the products. Mass spectral studies provide information regarding structural and molecular weight of a compound. The important IR stretching bands and molecular ion (M^+) peaks are depicted in Table 1.

3.2. Analysis of NMR spectra

The assignments of ^1H and ^{13}C NMR signals for compounds **9-16** are made with the help of 1D and 2D NMR spectra. Based on the ^1H NMR (D_2O exchange) spectra, the amine and amide NH protons are assigned. The DEPT-135 spectra are used to assist the assignment of ^{13}C NMR spectra. The characteristic ^1H and ^{13}C NMR signals of **9-16** are identified using 1D NMR spectra (^1H, ^{13}C and DEPT-135) and unambiguously assigned using 2D (COSY and HSQC) NMR spectra (Tables 2 & 3). While recording the ^1H NMR spectra of diazepan-5-ones **14-16** in DMSO-d_6, the amide NH protons appear as a doublet with the coupling constant value of 2-4.5 Hz which is due to the coupling between amide NH and proton at C-3. This observation suggests the migration of C-3 carbon during Schmidt rearrangement of piperidin-4-ones **1-8** to diazepan-5-ones **9-16**. The deshielding of C-3 carbon than C-6 in the ^{13}C NMR spectra of **9-16** also supports the above prediction.

*3.2.1. NMR spectral analysis of compound **9***

For the compound **9**, the two singlets at 1.92 and 6.13 ppm are assigned to amine and amide protons, respectively. Higher deshielding of amide proton is due to the presence of electron withdrawing C=O group and its resonance with nitrogen. Since no coupling partner is available at C-3 for C-2 proton, the H-2 benzylic proton appears as a singlet at 4.73 ppm. The chemical shift value of H-2 benzylic proton is comparable to that of 3-alkyl analogues which is indicative of the axial orientation for the proton and equatorial orientation for the aryl group at C-2.

The signal at 4.62 ppm appearing as doublet with ^{3}J value of 11.0 Hz ($^{3}J_{H6a,\ H7a}$) is assigned to the axial proton at C-7 (H-7a) which in turn confirms the equatorial position of the aryl group at C-7. Further, the signal at 4.62 ppm is correlated with a doublet of doublet at 3.10 ppm and a doublet at 2.69 ppm in its COSY spectrum (Fig. 1). This confirms that the peaks at 3.10 and 2.69 ppm are due to the axial and equatorial protons at C-6, respectively. The axial and equatorial protons can be assigned using their coupling constants. The signal at 3.10 shows coupling constants values of 11.5 and 15.0 Hz and the other one at 2.69 has the ^{2}J value of 15.5 Hz. The H-7a proton itself shows a doublet (^{3}J=11.0 Hz) instead of a doublet of doublet and the higher coupling constant value indicates that it is due to the diaxial coupling. Hence, the doublet of doublet at 3.10 ppm ($^{3}J_{H6a,\ H7a}$=11.5 Hz and $^{2}J_{H6a,\ H6e}$=15.0 Hz) and a doublet at 2.69 ppm ($^{2}J_{H6a,\ H6e}$ =15.5 Hz) are assigned to the axial and equatorial protons, H-6a & H-6e, respectively. The H-6e appears as a doublet instead of a doublet of doublet which indicates that it has zero coupling with H-7a, since the magnitude of the vicinal coupling approaches zero when the dihedral angle is 90°. The aromatic protons appear as multiplet between 7.18-7.69 ppm. The two methyl groups at C-3 appearing at 1.65 and 1.09 ppm are assigned to 3-CH_3 and 3-'CH_3, respectively. The assignments have been made for the other compounds **10-16** in a similar manner and the complete assignments of ^{1}H and ^{13}C NMR chemical shifts data are presented in Tables 2 and 3.

Correlation of protons with their coupling partners and one bond ^{1}H-^{13}C correlations are made unambiguously using ^{1}H-^{1}H COSY and ^{1}H-^{13}C HSQC, respectively (Fig. 1 and 2). ^{1}H-^{13}C HMBC NMR of **9** gives correlations between carbons and protons over longer ranges of about 2-4 bonds and the direct one-bond correlations are suppressed. By this the correlations of carbonyl and *ipso* carbons with ring protons can be understood. Two, three and four bond correlations are clearly depicted in Fig. 3. The complete correlation of ^{1}H-^{1}H COSY, ^{1}H-^{13}C HSQC and ^{1}H-^{13}C HMBC for **9** are presented in Table 4.

3.3. Conformational analysis

The preferred conformation of the diazepan-5-ones **9-16** has been arrived by considering the vicinal coupling constants between the H-7a and H-6a & H-6e protons as well as between H-2a and H-3a protons. The vicinal coupling constant data ($^3J_{H6a,\ H7a}$ and $^3J_{H6e,\ H7a}$) are employed to estimate the dihedral angles between the vicinal protons ($\Phi_{cis}=\Phi_{H6e,H7a}$ and $\Phi_{trans}=\Phi_{H6a,H7a}$) by DAERM [26] and are used for the conformational analysis. The extracted coupling constants and the estimated dihedral angles of **9-16** using DAERM are presented in Table 5. The conformations of several substituted piperidin-4-ones have been extensively studied in solution as well as in solid states which denote that the piperidine ring exists in a chair conformation with equatorial orientation of aryl groups [17, 27-29]. The extracted vicinal coupling constants and estimated dihedral angles for the reported piperidin-4-ones **6** and **7** are $J_{H2a,\ H3a}$= 10.3-10.5 Hz, $J_{H5a,\ H6a}$= 11.5 – 12.0 Hz, $J_{H5e,\ H6a}$= 2.3-3.0 Hz and Φ_{cis}= 57-60 ^{o}, Φ_{trans}=177-180 ^{o} [27].

The seven membered ring, in general, is more flexible than the six membered ring. Hence, the diazepan-5-one ring may not adopt rigid chair conformation like piperidin-4-ones. Here, the coupling constants and dihedral angles for diazepan-5-ones **9-16** are, $J_{H2a,\ H3a}$= 7.6-8.0 Hz, $J_{H6a,\ H7a}$= 10.8 - 11.6 Hz, $J_{H6e,\ H7a}$= 0 Hz and Φ_{cis}= 81 ^{o} & Φ_{trans}= 159 ^{o}. The *cis* coupling constant of 0 Hz observed between H-7a and H-6e in the diazepan-5-ones **9-16** suggests a dihedral angle close to 90^o. The dihedral angle of 81^o estimated using DAERM supports the above observation. The higher vicinal coupling constant values suggest that the aryl groups at C-2 and C-7 and the C-3 /C-6 alkyl groups of diazepan-5-ones **9-16** prefer to adopt the equatorial orientation. The observed values of coupling constants suggest that the diazepan-5-ones **9-16** adopts a chair conformation. Among the two methyl groups at C-3 for compounds **9-13**, one is axially oriented and the other one is equatorially oriented. The analysis of proton NMR data also reveals that H-6a is more deshielded than H-6e. Similarly the more deshielded methyl group (3-CH_3) is assigned as axial and the other methyl group (3-'CH_3) as equatorial.

3.4. Single crystal X-Ray studies

The ORTEP plots [30] of **9** and **11** are shown in Fig. 4. In **11**, there are two crystallographically independent molecules in the asymmetric unit with similar structural environment. The diazepine rings of **9** and **11** adopt distorted chair conformation (Fig. 5).

The puckering parameters [31] and asymmetry parameters [32] are: q2 = 0.277(2)Å, q3 = 0.676(2)Å, φ2 = 199.5(5)° & ΔCs(C-5) = 0.125.5(2)° for **9** and q2 = 0.309(2)Å[0.288(2)Å], q3 = 0.652(2)Å[0.665(2)Å], φ2 = 191.4(4)°[5.2(4)°] & ΔCs(C-5) = 113.4(2)°[0.120.8(2)°] for the molecule A[B] of **11**.

The planar phenyl rings substituted at C-2 and C-7 positions of the diazepine ring are in equatorial orientation in both **9** and **11** as evidenced from the torsion angles [(N4-C3-C2-C14/C5-C6-C7-C8) 168.67(2)°/159.2(2)° for **9**; -169.09(2)° & 165.82(2)° /161.46(2)° & -161.23(2)° for the two molecules in **11**]. The best plane of diazepine ring orients at angles of 60.59(11)° and 70.59(11)° with respect to the phenyl rings of **9** and 62.74(11)° & 60.14(9)° (molecule A) and 73.76(9)° & 65.29(1)° (molecule B) of **11**, respectively.

In **9** & **11**, one of the methyl groups (C-20) substituted at C-3 occupies equatorial orientation whereas the other (C-21) occupies axial orientation (N1-C2-C3-C20/ N1-C2-C3-C21 -175.68(18)°/-53.8(2)° for **9**; -175.13(16)° & 174.52(18)°/-53.7(2)° & 52.1(2)° for **11**. The chlorine atom and methyl group in both the molecules of **9** and **11** lie in the plane of phenyl rings which is evidenced from the deviation from the attached rings (0.014(1)Å & -0.060(1)Å of Cl-1 & Cl-2 for **9**; -0.009(4)Å[0.033(3)Å] & 0.096(4)Å[0.038(3)Å]C-22 C-23 For **11**(A[B]). In **9** and **11**, the molecules are stabilized by N-H...O, C-H...Cl and C-H...N types of hydrogen bondings. In both the compounds the molecules are linked through N-H...O hydrogen bond into cyclic centrosymmetric R^2_2 dimer [33] as shown in Fig. 6.

3.5. Docking Analysis

Methicillin-resistant Staphylococcus aureus (MRSA) is gram-positive human bacterial pathogen which is highly connected with infections in hospitals. It is acquiring resistance to the β-lactam antibiotics and vancomycin [34], which necessitates the search to find alternative drugs. The structural information retrieved from the "Protein Data Bank" (PDB ID: 4D7I) has been used as the template for this study. The diazepanones **9**-**16** are shown to be effective inhibitor against MRSA. X-ray crystal structures have been utilized to predict the expected binding mode and electronic properties enabled optimization to diazepanones as a potent second-generation lead. The results obtained from this study would be useful in both understanding the inhibitory mode of diazepan-5-ones **9**-**16** and accurately predicting the activities of newly designed inhibitors on the basis of docking scores. These models also provide some beneficial clues in structural modification for designing new drug.

A view of the X-ray crystal structure of the MRSA active site shows the key hydrogen contacts between co-crystal [6-(4-(((3-fluorophenethyl)amino)methyl)phenyl)-4-methylpyridin-2-amine] and enzyme and this is illustrated in Fig. 7. The surface diagrams for eight diazepanone molecules docked at the active site of MRSA are depicted in Fig. 8. The molecules predominantly interact with Glu243 target residue, in the docked pose of MRSA. Scaffolds containing methoxy substituted phenyl rings in the structure are placed well into the pocket lined by hydrophobic residues; the polar heads bearing carbonyl and hydroxyl groups interact through H-bonds with the polar side chains of the amino acids at the active site. Molecules **13** and **14** show more number of H-bond interactions at the active site residues. Among them, following interactions Glu243, Tyr239, His128, Asp220, Arg132, Gln129, Trp329 and Asn248 have also been noticed in the co-crystal ligand of MRSA, apart from this, interaction with other residues like Trp59, Leu162, Val163, Lys200, Ile235, Glu240 and Asp300 has been found in remaining compounds. Overall, molecule **10** [2,7-bis(4-chlorophenyl)-3,3-dimethyl-1,4-diazepan-5-one] is having better docking score and glide energy is comparable to co-crystal ligand of MRSA. The docking score, glide energy and hydrogen bonding interactions are presented along with the co-crystal ligand (Fig. 9. & Table 6) docked at the active site of target for all molecules. The results indicate that the identified compounds have good and efficient inhibitory activities against the chosen target.

3.6. Antibacterial activity assay

All the synthesized compounds **9-16** have been screened for antibacterial activity against four bacterial strains using agarose well diffusion method and by minimum inhibitory concentration (MIC) method [23, 24]. The solvent, DMSO used for the preparation of compounds does not show inhibition against the tested organisms. The results reveal that most of the synthesized compounds exhibit antibacterial activity against *S. aureus*, *S. pyogenes*, and *E. coli* whereas *M. luteus* strain shows no activity. The results are presented in Tables 7 & 8. Compounds **10**, **11**, **15** and **16** dictate a certain degree of antibacterial activity except *M. luteus*. Moreover, compounds **11** and **15** show better activity among the all compounds.

The minimal inhibitory concentration has been screened by MTT assay method [24]. Here, DMSO has been used as a negative control and ampicillin as a positive control. Among all the compounds **9-16**, only the compound **11** shows comparable results with the standard drug ampicillin against *S. aureus* and *E. coli* strains. The other compounds show

significant to weak bactericidal inhibitory activity against *S. aureus*, *S. pyogenes*, *E. coli* and *M. luteus*. All the compounds **9-16** exhibit better activity against *S. aureus* when compared with other strains.

3.7. Antioxidant activity

The DPPH radical scavenging method [25] is the most common tool to inspect the antioxidant capacity of the specific compounds. The synthesized compounds **9-16** interact with the free radicals in the DPPH and inhibit the oxidation exhibiting a certain degree of radical scavenging activity. The antioxidant results are expressed in terms of IC_{50} in µM as presented in Table 9. From the results, the compounds **11** (24.68 ± 0.48), **13** (30.29 ± 0.29) and **14** (26.90 ± 0.39) show significant antioxidant activities equal to half of the antioxidant power of standard BHT. All the remaining compounds exhibit moderate antioxidant activity. In general, presence of electron donating groups in the aromatic ring of compounds **11** (4-CH_3) and **13** (4-OCH_3) show better antioxidant activity than the electron withdrawing groups in the aromatic rings of compounds **9** (2-Cl) and **10** (4-Cl). The compound having Cl at the *ortho* position of the aromatic ring (**9**) shows higher activity than the Cl at the *para* position (**10**). The increase in bulkiness of groups at the C-3 carbon of the diazepanone ring results in the decrease of antioxidant activity (**14**>**15)**. The substituted aromatic rings show batter activity than the unsubstituted phenyl rings (**9-11**, **13** and **14**> **12**). Among the diazepanones **9-16**, the antioxidant activity order can be presented as **11**> **14**> **13**> **9**> **10**> **12**> **16**> **15**.

4. Conclusion

In summary, diazepan-5-ones **9-16** have been synthesized using Schmidt rearrangement in good yields by adopting simple one step procedure. All the compounds are characterized using IR, mass, 1D and 2D NMR spectral studies. The stereochemistry of compounds **9-16** has been studied with the help of ^{1}H and ^{13}C NMR data. The diazepan-5-ones **9-16** prefer to adopt chair conformation with equatorial orientation of alkyl groups at C-3/C-6 and aryl groups at C-2 and C-7. Single crystal X-ray diffraction studies have been carried out for the compounds **9** and **11** which show the preference for distorted chair conformation with equatorial orientation of substituents. The *in silico* docking study has been carried out for all the compounds which reveals the better docking score of the compound **10** and the comparable glide energy to co-crystal ligand of MRSA. The *in vitro* evaluation of antibacterial activities reveal that the compound **11** has better activity against *S. aureus* and *E. coli* strains and the remaining compounds exhibit moderate activity when

compared with standard drug ampicillin. The compounds **11**, **13** and **14** exhibit the activity equal to half of the antioxidant power of standard drug and the remaining compounds show moderate activity, as seen from the antioxidant assay.

Acknowledgements

SS thanks UGC, New Delhi for the award of Rajiv Gandhi National Fellowship (RGNFS). PS thanks the UGC, New Delhi for the financial support in the form of a Research Fellowship in Science for Meritorious Students. We wish to thank (SAIF) IIT, Chennai and (SIF) Vellore for NMR spectra.

Additional information

Crystallographic data (CIF and FCF) for the structures of compounds **9** and **11** reported in this paper have been deposited with the Cambridge Crystallographic Data Centre as supplementary publication numbers, CCDC 1442870 and CCDC 1442857, respectively. Copies of the data can be obtained free of charge, on application to CCDC, 12 Union Road, Cambridge CB2 1 EZ, UK. (fax: +44-(0)1223-336033 or email: deposit@ccdc.cam.ac.uk).

References

[1] E. Tarkin-Tas, L.J. Mathias, Macromolecules, 43 (2010) 968-974.

[2] J. Ramos, A. Imaz, J. Forcada, Polym. Chem., 3 (2012) 852-856.

[3] K.S.K. Murthy, E.E. Knaus, Drug Dev. Res., 46 (1999) 155-162.

[4] M. Gopalakrishnan, P. Sureshkumar, J. Thanusu, V. Kanagarajan, R. Govindaraju, G. Jayasri, J. Enzyme Inhib. Med. Chem., 22 (2007) 709-715.

[5] V. Wolkinger, R. Weis, F. Belaj, M. Kaiser, R. Brun, R. Saf, W. Seebacher, Aust. J. Chem., 62 (2009) 1166-1172.

[6] V. Baliah, M. Lakshmanan, K. Pandiarajan, Indian J. Chem., 16B (1978) 72-73.

[7] M. Gopalakrishnan, P.S. Kumar, J. Thanusu, C. Prabhu, V. Kanagarajan, J. Chem. Res., (2007) 80-81.

[8] U.P. Senthilkumar, R. Jeyaraman, R.W. Murray, M. Singh, J. Org. Chem., 57 (1992) 6006-6014.

[9] R. Jeyaraman, U.P. Senthilkumar, P. Bigler, J. Org. Chem., 60 (1995) 7461-7470.

[10] R. Jeyaraman, S. Ponnuswamy, J. Org. Chem., 62 (1997) 7984-7990.

[11] S. Thennarasu, P.T. Perumal, Molecules, 7 (2002) 487-493.

[12] S. Sethuvasan, M.Phil. Dissertation, Bharathiar University, India, (2009).

[13] K. Ravichandran, P. Ramesh, S. Sethuvasan, S. Ponnuswamy, M.N. Ponnuswamy, Acta Cryst., E65 (2009) o2884.

[14] K. Ravichandran, P. Ramesh, S. Sethuvasan, S. Ponnuswamy, M.N. Ponnuswamy, Acta Cryst., E65 (2009) o2885-o2886.

[15] S. Ponnuswamy, A. Akila, D. Kiruthiga Devi, Synth. Commun., 45 (2015) 2030-2034.

[16] V. Maheshwaran, S. Sethuvasan, K. Ravichandran, S. Ponnuswamy, P. Sugumar, M.N. Ponnuswamy, Chem. Cent. J., 9 (2015) 17.

[17] S.S. Ilango, S. Ponnuswamy, T. Viswanathan, Indian J. Heterocycl. Chem., 20 (2010) 17-20.

[18] A. Bruker, SAINT and SADABS, Bruker Analytical X-ray Systems, Inc., Madison, Wisconsin, USA, (2008).

[19] G.M. Sheldrick, Acta cryst., A64 (2008) 112-122.

[20] S.K. J.K. Holden, F.C. Beasley, M.A. Cinelli, H. Li, S.G. Roy, D. Dejam, A.L. Edinger, V. Nizet, R.B. Silverman, T.L. Poulos, Chem. Biol., 22 (2015) 758-792.

[21] Schrödinger, Maestro, version 9.8; Schrödinger, LLC: New York, 2014.

[22] W.L. Delano, The PyMOL Molecular Graphics System, 2002.

[23] A. Sen, A. Batra, Int. J. Curr. Pharm. Res., 4 (2012) 67-73.

[24] T. Mosmann, J. Immunol. Methods, 65 (1983) 55-63.

[25] M.S. Blois, Nature, 29 (1958) 1199-1200.

[26] K.N. Slessor, A.S. Tracey, Can. J. Chem., 49 (1971) 2874-2884.

[27] P. Sakthivel, S. Ponnuswamy, J. Mol. Struct., 1074 (2014) 349-358.

[28] S. Ponnuswamy, V. Mohanraj, S.S. Ilango, M. Thenmozhi, M.N. Ponnuswamy, J. Mol. Struct., 1081 (2015) 449-456.

[29] S. Ponnuswamy, S. Sethuvasan, K. Thirunavukarasu, J. Mol. Struct., 1089 (2015) 86-94.

[30] L. Farrugia, J. Appl. Crystallogr., 30 (1997) 565.

[31] D. Cremer, J.A. Pople, J. Am. Chem. Soc., 97 (1975) 1354-1358.

[32] M. Nardelli, Acta Cryst., C39 (1983) 1141-1142.

[33] J. Bernstein, R.E. Davis, L. Shimoni, N.L. Chang, Angew. Chem. Int. Ed. (English), 34 (1995) 1555-1573.

[34] P. Loomba, J. Taneja, B. Mishra, J. Global Infect. Dis., 2 (2010) 275-283.

All captions

Scheme 1

Synthesis of *r*-2,*c*-7-diaryl[1,4]diazepan-5-ones **9-16**.

Figure captions

Figure 1

^{1}H-^{1}H COSY NMR spectrum of **9**.

Figure 2

^{1}H-^{13}C HSQC NMR spectrum of **9**.

Figure 3

^{1}H-^{13}C HMBC NMR spectrum of **9**.

Figure 4

The ORTEP plot of the molecules **9** and **11**.

Figure 5

Chair conformation of compounds **9** and **11**.

Figure 6

Crystal packing of compounds **9** and **11**.

Figure 7

Interaction of protein with the co-crystal

Figure 8

Surface diagram showing the binding of **9-16** within the hydrophobic pocket of MRSA.

Figure 9

Interactions of **9-16** docked complex with MRSA.

Table captions

Table 1

Analytical data of diazepan-5-ones **9**-**16**

Table 2

^{1}H NMR chemical shift values of diazepan-5-ones **9**-**16** [δ (ppm)]

Table 3

^{13}C NMR chemical shift values of diazepan-5-ones **9**-**16** [δ (ppm)]

Table 4

^{1}H-^{1}H COSY, ^{1}H-^{13}C HSQC and ^{1}H-^{13}C HMBC correlations of **9**

Table 5

Coupling constants (Hz) and dihedral angles (°) of compounds **9**-**16**

Table 6

Hydrogen bond interactions of **9**-**16** and co-crystallized ligand with amino acids at the active site of MRSA

Table 7

Zone of inhibition in mm at 100 µg/ml concentration of **9**-**16** with selected bacterial strains

Table 8

Minimum inhibitory concentration (MIC) of **9**-**16** against selected bacterial strains

Table 9

Screening results of DPPH radical scavenging activity of **9**-**16**.

Table 1

compound	Molecular weight	m.p. (ºC)	Yield (%)	Elemental analysis Found (Calcd) %			IR stretching frequencies (cm^{-1})		
				C	H	N	NH (amine)	NH (amide)	C=O (amide)
9	363.49	284-286	72	62.47 (62.82)	5.66 (5.55)	8.08 (7.71)	3288	3204	1654
10	363.58	202-204	69	63.08 (62.82)	5.64 (5.55)	7.39 (7.71)	3282	3198	1652
11	322.73	144-146	75	77.94 (78.22)	8.27 (8.13)	9.01 (8.69)	3281	3203	1651
12	294.00	208-210 [Lit.[6] 210]	81	-	-	-	3285	3195	1668
13	354.18	172-174	71	71.50 (71.16)	7.28 (7.39)	8.26 (7.90)	3285	3216	1653
14	340.12	180-182	69	70.79 (70.56)	7.26 (7.11)	8.51 (8.23)	3322	3202	1666
15	354.10	138-140	70	71.42 (71.16)	7.24 (7.39)	8.21 (7.90)	3307	3214	1673
16	354.23	133-135	68	70.83 (71.16)	7.47 (7.39)	7.64 (7.90)	3294	3206	1666

Table 2

Compound	H-2a	H-3a	H-6a	H-6e	H-7a	3-CH_3	3-'CH_3	3-CH_2CH_3	6-CH_3	C-4'/C-4'' OCH_3	C-4'/C-4'' CH_3	NH	CONH	Aromatic protons
9	4.73 (s)	-	3.10 (dd)	2.69 (d)	4.62 (d)	1.65 (s)	1.09	-	-	-	-	1.92 (br.s)	6.13 (s)	7.69-7.18 (m)
10	3.93 (s)	-	3.11 (dd)	2.58 (d)	4.08 (d)	1.57 (s)	0.96	-	-	-	-	1.90 (br.s)	6.30 (s)	7.38-7.26 (m)
11	3.90 (s)	-	3.14 (dd)	2.62 (d)	4.06 (d)	1.58 (s)	0.94	-	-	-	2.30 (s)	1.89 (br.s)	6.11 (s)	7.31-7.06 (m)
12	3.87 (s)	-	3.09 (dd)	2.56 (d)	4.03 (d)	1.53 (s)	0.88	-	-	-	-	1.88 (br.s)	6.21 (s)	7.36-7.17(m)
13	3.89 (s)	-	3.13 (dd)	2.60 (d)	4.05 (d)	1.57 (s)	0.94	-	-	3.78, 3.77 (s)	-	1.86 (br.s)	5.95 (s)	7.35-6.80 (m)
14	3.64 (s)	a	3.10 (dd)	2.61 (dd)	4.07 (d)	0.81 (d)	-	-	-	a	-	1.96 (br.s)	5.91 (s)	7.33-6.82 (m)
15	3.71 (s)	3.58 (m)	3.10 (dd)	2.61 (dd)	4.08 (d)	-	-	1.09 (m, CH_2), 0.85 (m, CH_3)	-	3.78, 3.77 (s)	-	1.97 (br.s)	5.71 (s)	7.33-6.82 (m)
16	3.61 (s)	b	3.04 (dd)	-	b	0.81 (d)	-	-	0.72 (d)	b	-	2.00 (br.s)	5.75 (s)	7.30-6.81 (m)

(a) 3.80-3.75 (δ, ppm) H-3a merged with C-4'/C-4''OCH_3, (b) 3.80-3.74 (δ, ppm) H-3a and H-7a merged with C-4'/C-4''OCH_3

Table 3

Compound	C-2	C-3	C-5	C-6	C-7	3-CH_3	3-'CH_3	3-CH_2CH_3	6-CH_3	C-4'/C-4'' OCH_3	C-4'/C-4'' CH_3	Aromatic *ipso* carbons	Aromatic carbons
9	67.41	56.68	174.65	45.05	56.78	21.93	28.39	-	-	-	-	141.29, 139.65, 133.99, 132.59	129.81, 129.71, 128.89, 128.79, 128.74, 127.29, 127.14, 127.04
10	73.08	55.80	174.58	46.84	60.38	21.31	30.41	-	-	-	-	142.86, 140.29, 133.87, 133.54	129.55, 128.97, 128.48, 127.75
11	73.69	56.16	175.32	47.12	60.96	21.54	30.54	-	-	-	21.14, 21.10	141.92, 139.34, 137.60, 137.38	129.39, 128.88, 128.24, 126.36
12	73.87	56.02	175.18	47.06	61.17	21.45	30.41	-	-	-	-	144.65, 142.12	128.72, 128.34, 128.21, 127.92, 127.75, 126.43
13	73.17	56.16	175.19	47.03	60.55	21.37	30.56	-	-	55.29, 55.25	-	159.18, 159.05, 137.05, 134.42	129.27, 127.45, 114.02, 113.49
14	70.45	54.91	175.83	47.59	59.03	19.90	-	-	-	55.27, 55.26	-	159.23, 159.00, 137.23, 134.59	128.65, 127.86, 127.48, 113.96, 113.91, 113.70
15	69.44	59.14	176.18	47.56	60.69	-	-	25.72 (CH_2), 10.06 (CH_3)	-	55.41, 55.27, 55.25	-	159.21, 159.00, 137.29, 134.39	129.32, 128.73, 127.47, 114.22, 113.95, 113.93, 113.78
16	70.45	54.40	178.49	46.07	64.43	19.71	-	-	14.60	55.25	-	159.20, 158.99, 135.67, 134.70	128.83, 128.65, 113.87, 113.66

Table 4

Chemical shift (δ, ppm)	^{1}H-^{1}H COSY	^{1}H-^{13}C HSQC	^{1}H-^{13}C HMBC
H-2a, 4.73 (s, 1H)	-	67.41 (C-2)	21.93 (3-CH_3), 56.68 (C-3), 132.59 (C-2'), 139.65 (C-1'), 174.65 (CONH)
H-6a, 3.10 (dd, 1H)	H-6e, H-7a	45.05 (C-6)	56.78 (C-7), 174.65 (CONH)
H-6e, 2.69 (d, 1H)	H-6a	45.05 (C-6)	56.78 (C-7), 141.29 (C-1''), 174.65 (CONH)
H-7a, 4.62 (d, 1H)	H-6a	56.78 (C-7)	67.41 (C-2), 132.59 (C-2''), 141.29 (C-1'')
3-CH_3, 1.65 (s, 3H)	-	21.93 (3-CH_3)	28.39 (3-'CH_3), 56.68 (C-3), 67.41 (C-2)
3-'CH_3, 1.09 (s, 3H)	-	28.39 (3-'CH_3)	21.93 (3-CH_3), 56.68 (C-3), 67.41 (C-2), 174.65 (CONH)

Table 5

Compound	coupling constants (Hz)				Dihedral angles (°)	
	$^{3}J_{H2a, H3a}$	$^{2}J_{H6a, H6e}$	$^{3}J_{H6a, H7a}$	$^{3}J_{H6e, H7a}$	$\Phi_{H6e,H7a}$	$\Phi_{H6a,H7a}$
9	-	15.0	11.5	0	81	159
10	-	15.2	11.6	0	81	159
11	-	15.2	11.6	0	81	159
12	-	15.5	11.5	0	81	159
13	-	15.2	11.6	0	81	159
14	8.0	14.0	10.8	0	81	159
15	7.6	14.0	10.8	0	81	159
16	8.0	-	-	-	-	-

Table 6

Compounds	Glide Score	Glide Energy (kcal/mol)	Hydrogen Bonding	
			Interactions	**Distance (Å)**
Co-Crystal (PDB ID: 4D7I)	-7.52011	-49.9386	N-H…O(GLU243 N-H…O(TYR357)	2.9 3.8
9	-6.79254	-55.1623	-	-
10	-7.86139	-57.6659	O…H-O(TYR357) O…H-N(ARG247)	2.87 2.93
11	-6.3959	-50.2444	O…H-N(ARG247) N-H…N(ARG247)	3.4 2.8
12	-8.24083	-51.0804	N-H…O(HEM901) O-H…O(HEM901)	3.2 3.4
13	-7.00516	-47.7864	O…H-O(GLU243) O…H-N(GLN129) O-H…O(HIS128) N-H…O(ASP220) N-H…O(HEM901) O…H-N(ARG132)	2.8 2.9 2.8 3.3 3.0 3.0
14	-7.53081	-48.6479	O-H…O(TYR239) O…H-N(TRP329 N-H…O(ASN248) O…H-N(ASN248) N-H…O(GLU243) N…H-N(ARG132)	3.0 2.8 3.2 2.8 3.0 3.4
15	-7.48146	-49.2091	O…H-N(ARG132) O…H-O(GLU243) O-H…O(HEM901)	3.3 2.9 2.7
16	-8.16355	-49.199	O…H-O(GLU243) O-H…O(ASP220) O…H-N(HIS128) N-H…O(HEM901)	2.5 2.8 3.1 3.2

Table 7

Cpds	Diameter of inhibition zone (mm)			
	S. aureus	***S. pyogenes***	***M. luteus***	***E.coli***
9	12.29 ± 0.73	-	-	-
10	10.92 ± 0.45	10.11 ± 0.32	-	11.65 ± 0.27
11	16.19 ± 0.32	11.12 ± 0.34	-	14.16 ± 0.71
12	-	-	-	-
13	-	-	-	10.29 ± 0.33
14	10.29 ± 0.69	11.72 ± 0.22	-	-
15	14.48 ± 0.26	16.95 ± 0.35	-	10.19 ± 0.51
16	11.11 ± 0.38	11.09 ± 0.29	-	11.43 ± 0.95
Ampicillin	24.12 ± 0.23	28.63 ± 0.31	-	22.43 ± 0.65

Table 8

Cpds	IC_{50} Concentration µM			
	S. aureus	***S. pyogenes***	***M. luteus***	***E. coli***
9	60.72 ± 0.31	95.97 ± 0.13	97.68 ± 0.34	92.88 ± 0.34
10	64.91 ± 0.18	93.69 ± 0.34	93.99 ± 0.18	88.02 ± 0.08
11	25.85 ± 0.07	70.74 ± 0.17	80.14 ± 0.06	31.63 ± 0.21
12	87.00 ± 0.27	82.05 ± 0.29	85.57 ± 0.21	83.77 ± 0.17
13	70.42 ± 0.33	87.81 ± 0.17	101.91 ± 0.13	84.28 ± 0.20
14	64.46 ± 0.28	81.21 ± 0.20	93.81 ± 0.32	64.45 ± 0.11
15	45.63 ± 0.33	75.94 ± 0.23	89.91 ± 0.20	81.08 ± 0.35
16	61.73 ± 0.17	81.21± 0.08	100.28 ± 0.12	74.46 ± 0.17
Ampicillin	18.57 ± 0.19	17.02 ± 0.15	24.15 ± 0.34	19.87 ± 0.26

Table 9

Compounds	DPPH (IC_{50} ± SD[a]) µM
9	64.96 ± 0.50
10	77.80 ± 0.83
11	24.68 ± 0.48
12	87.73 ± 0.36
13	30.29 ± 0.29
14	26.90 ± 0.39
15	135.86 ± 0.91
16	124.83 ± 0.38
BHT	12.46 ± 0.12

[a] The results are average of triplicate analysis. Lower IC_{50} values indicate higher radical scavenging activity.

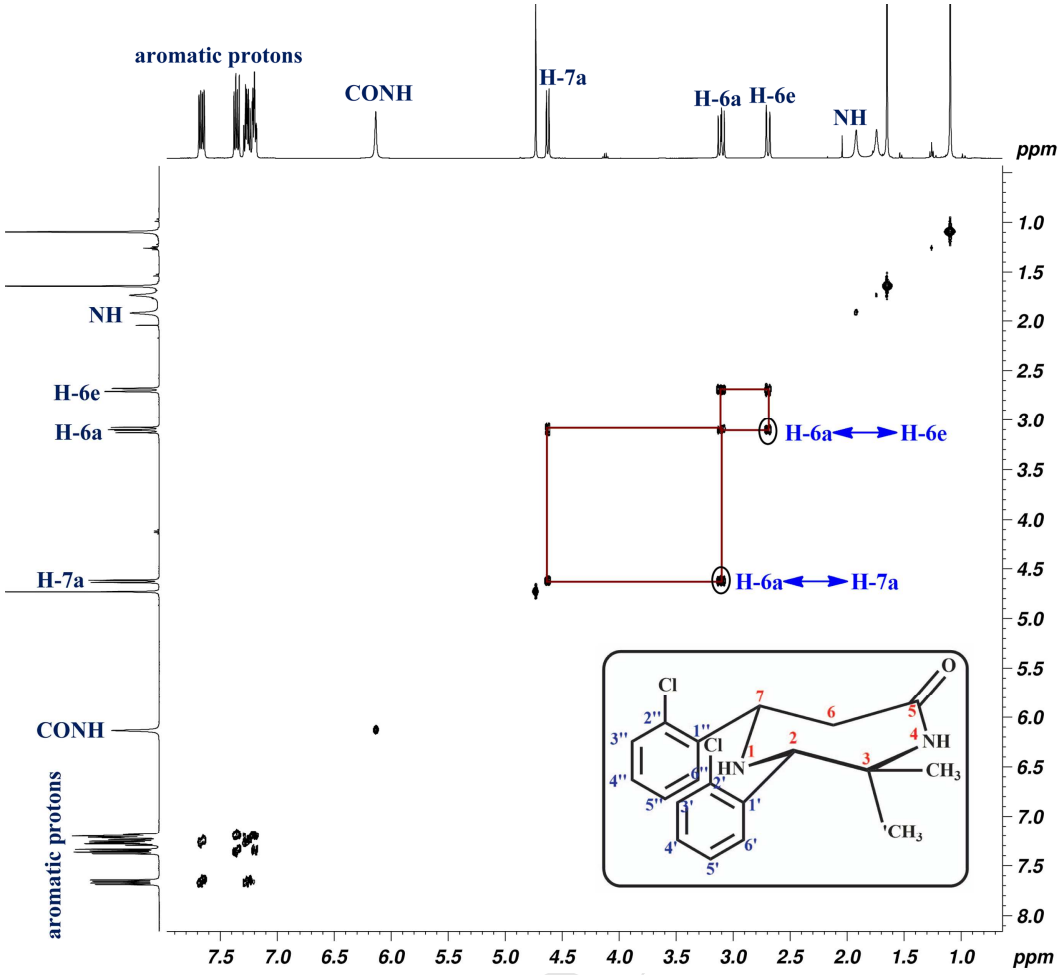
aromatic protons
CONH
H-7a
H-6a
H-6e
NH
ppm
NH
H-6e
H-6a
H-7a
CONH
aromatic protons
H-6a↔H-6e
H-6a↔H-7a
Cl
Cl
HN
O
NH
CH3
'CH3
7.5 7.0 6.5 6.0 5.5 5.0 4.5 4.0 3.5 3.0 2.5 2.0 1.5 1.0 ppm

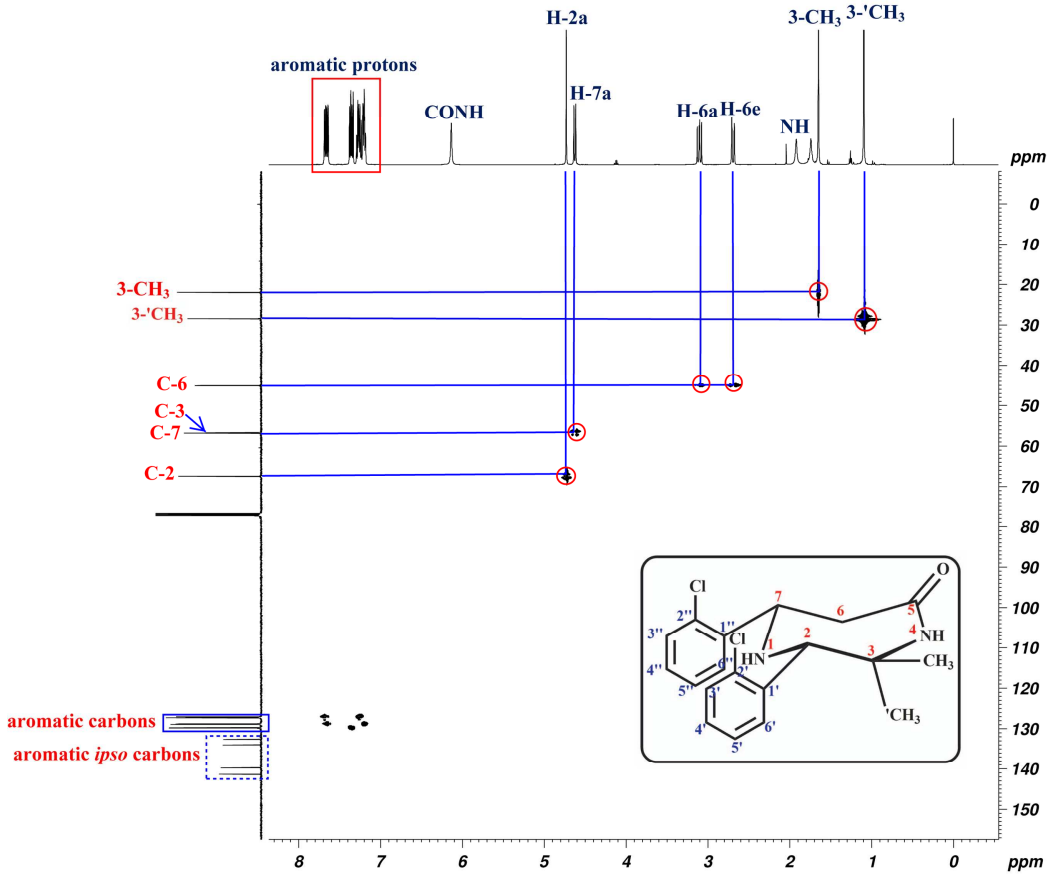

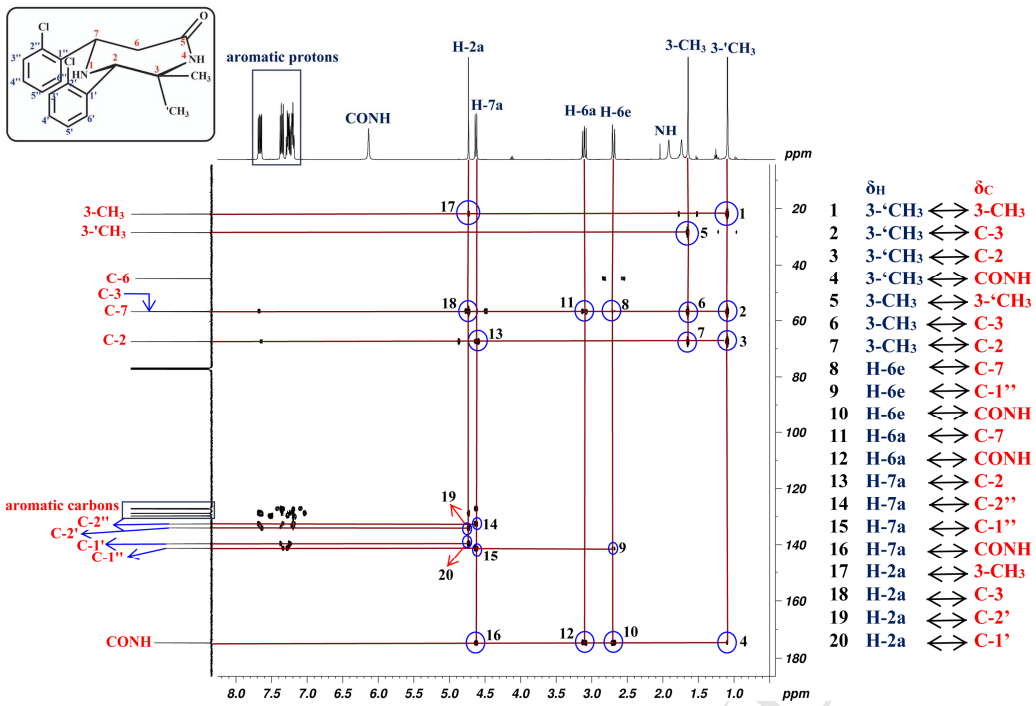

	δ_H		δ_C
1	3-‘CH_3	⟷	3-CH_3
2	3-‘CH_3	⟷	C-3
3	3-‘CH_3	⟷	C-2
4	3-‘CH_3	⟷	CONH
5	3-CH_3	⟷	3-‘CH_3
6	3-CH_3	⟷	C-3
7	3-CH_3	⟷	C-2
8	H-6e	⟷	C-7
9	H-6e	⟷	C-1’’
10	H-6e	⟷	CONH
11	H-6a	⟷	C-7
12	H-6a	⟷	CONH
13	H-7a	⟷	C-2
14	H-7a	⟷	C-2’’
15	H-7a	⟷	C-1’’
16	H-7a	⟷	CONH
17	H-2a	⟷	3-CH_3
18	H-2a	⟷	C-3
19	H-2a	⟷	C-2’
20	H-2a	⟷	C-1’

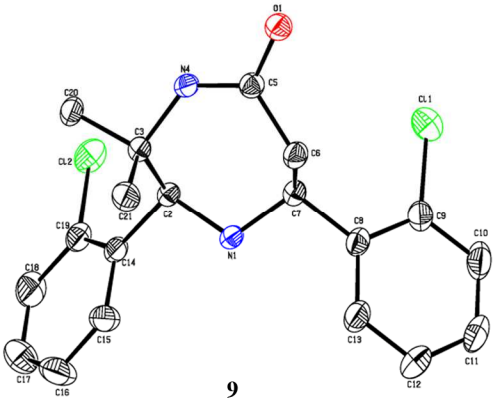

9

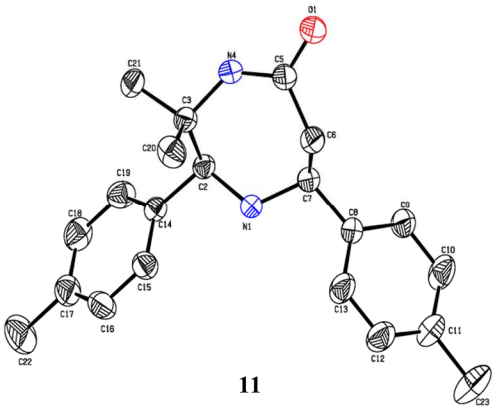

11

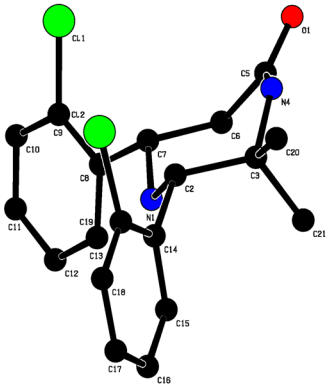

9

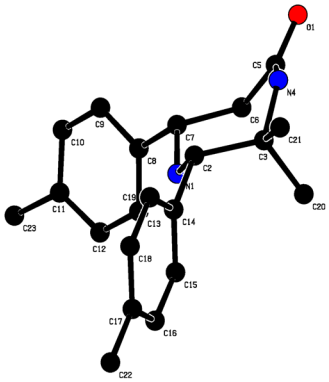

11

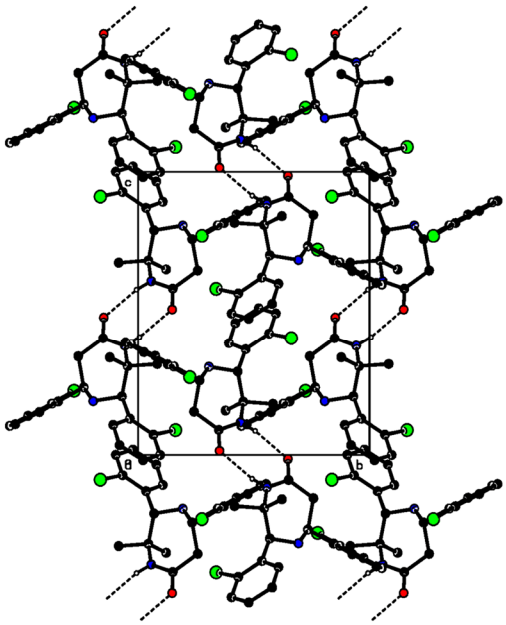

9

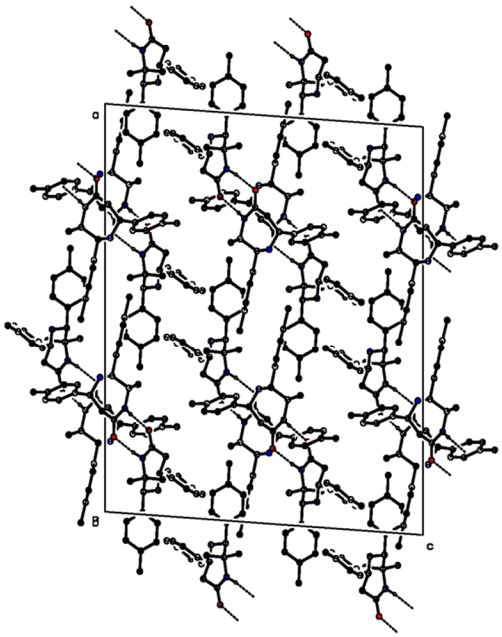

11

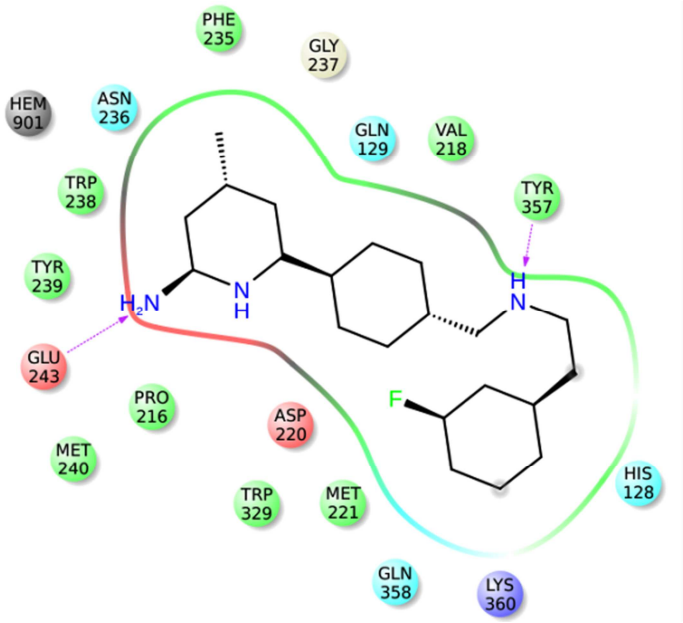

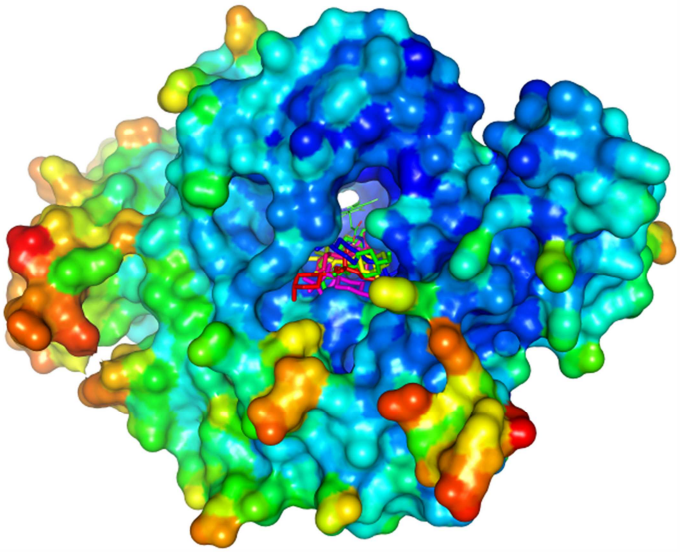

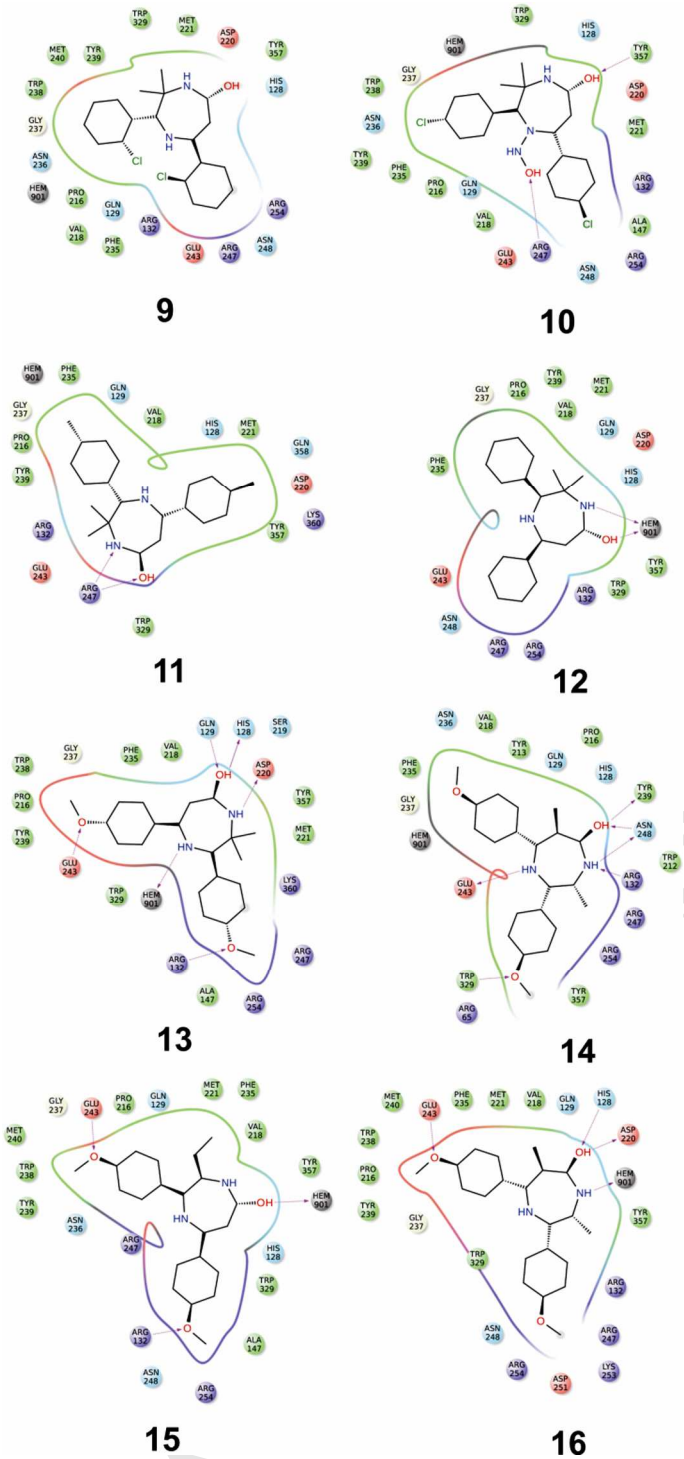

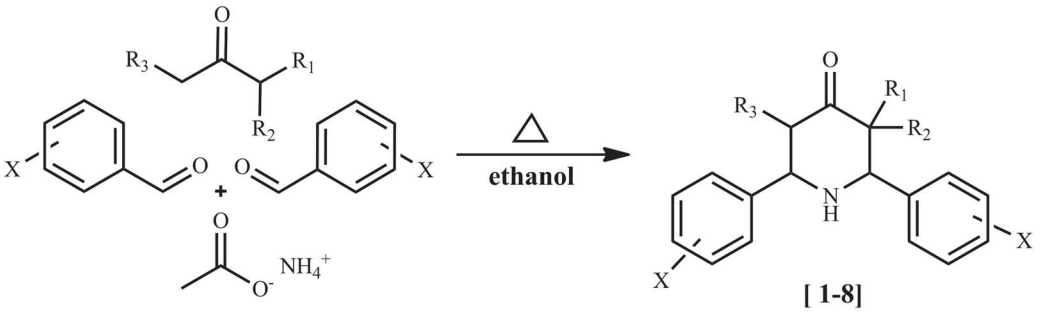

conc. HCl/ DCM | conc. H_2SO_4/NaN_3

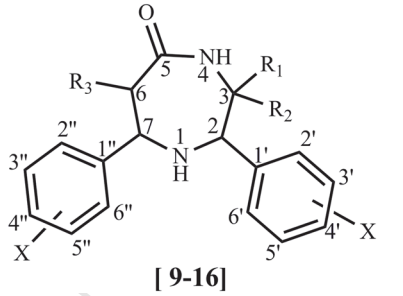

Entry	R_1	R_2	R_3	X
9	CH_3	CH_3	H	2-Cl
10	CH_3	CH_3	H	4-Cl
11	CH_3	CH_3	H	4-CH_3
12	CH_3	CH_3	H	H
13	CH_3	CH_3	H	4-OCH_3
14	CH_3	H	H	4-OCH_3
15	C_2H_5	H	H	4-OCH_3
16	CH_3	H	CH_3	4-OCH_3

Highlights

- ✓ Seven new diazepan-5-ones have been synthesized and characterized using NMR spectra
- ✓ X-ray crystal structures have been solved for compounds **9** and **11**
- ✓ Diazepan-5-ones adopt chair conformation in solution and solid states
- ✓ Docking studies confirm the binding of active compounds with MRSA
- ✓ Compounds have been evaluated for their antibacterial and antioxidant activities